Supplementary Figures

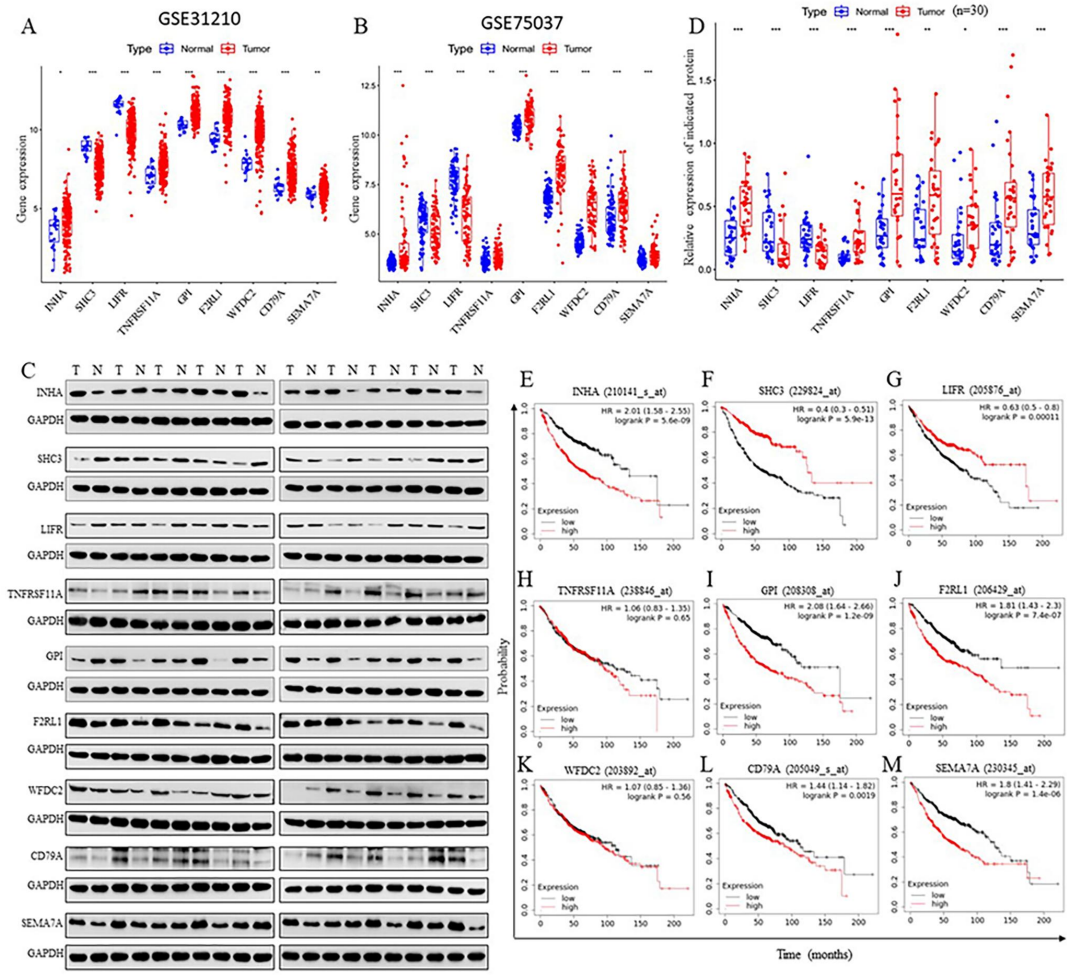

Figure S1. The expression level of nine prognostic signature genes in LUAD and prognostic value for LUAD. (A, B) The mRNA expression levels of INHA, SHC3, LIFR, TNFRSF11A, GPI, F2RL1, WFDC2, CD79A, and SEMA7A were estimated using GSE31210 (A) and GSE75037 (B) datasets. (C, D) Representative Western blotting analysis of the expression levels of these nine signature genes in 30 paired LUAD tissues and adjacent tissues (C). The quantitative results of grayscale scanning were shown using GAPDH as the loading control (D). (E-M) Survival analysis of signature genes for LUAD. LUAD patients were subdivided into low/high gene expression groups according to the median expression level of each gene in LUAD tissues. O.S. analysis of INHA (E), O.S. analysis of SHC2 (F), O.S. analysis of LIFR (G), O.S. analysis of TNFRSF11A (H), O.S. analysis of GPI (I), O.S. analysis of F2RL1 (J), O.S. analysis of WFDC2 (K), O.S. analysis of CD79A (L) and O.S. analysis of

SEMA7A (M). T, tumor tissue; N, normal tissue. HR, hazard ratio. *, *P*<0.05; **, *P*<0.01; ***, *P*<0.001.

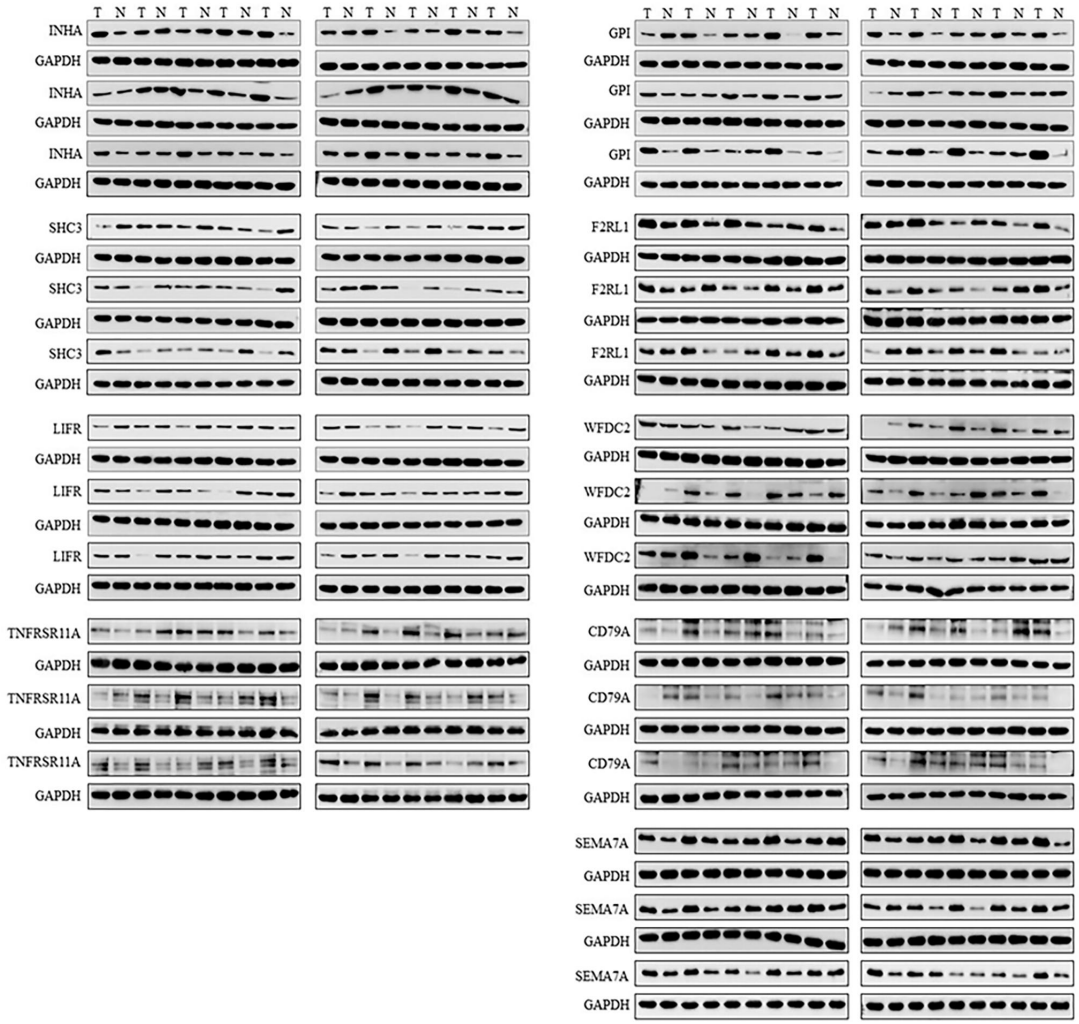

Figure S2. **The expression levels of nine prognostic signature genes in 30 paired LUAD tissues and adjacent tissues were evaluated by Western blotting analysis.**

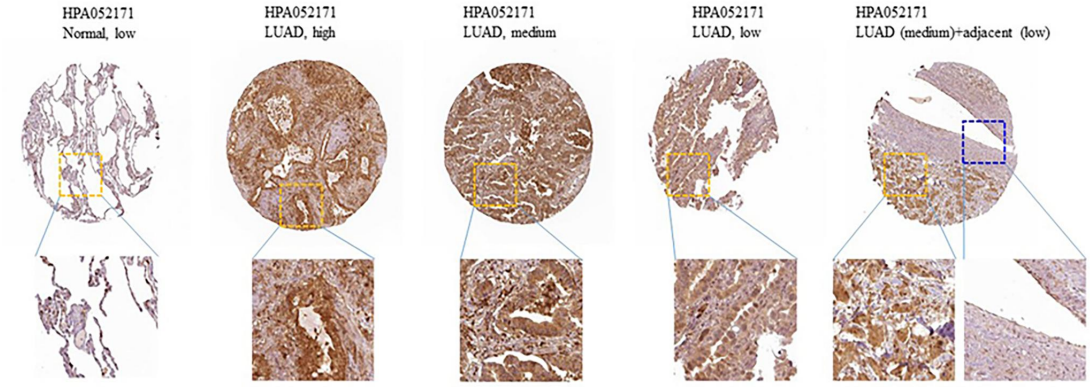

Figure S3. The expression characteristics of prognostic signature gene GPI and its correlation with LUAD based on immunohistochemistry analysis using the Human Protein Altas (HPA) database. LUAD, lung adenocarcinoma.

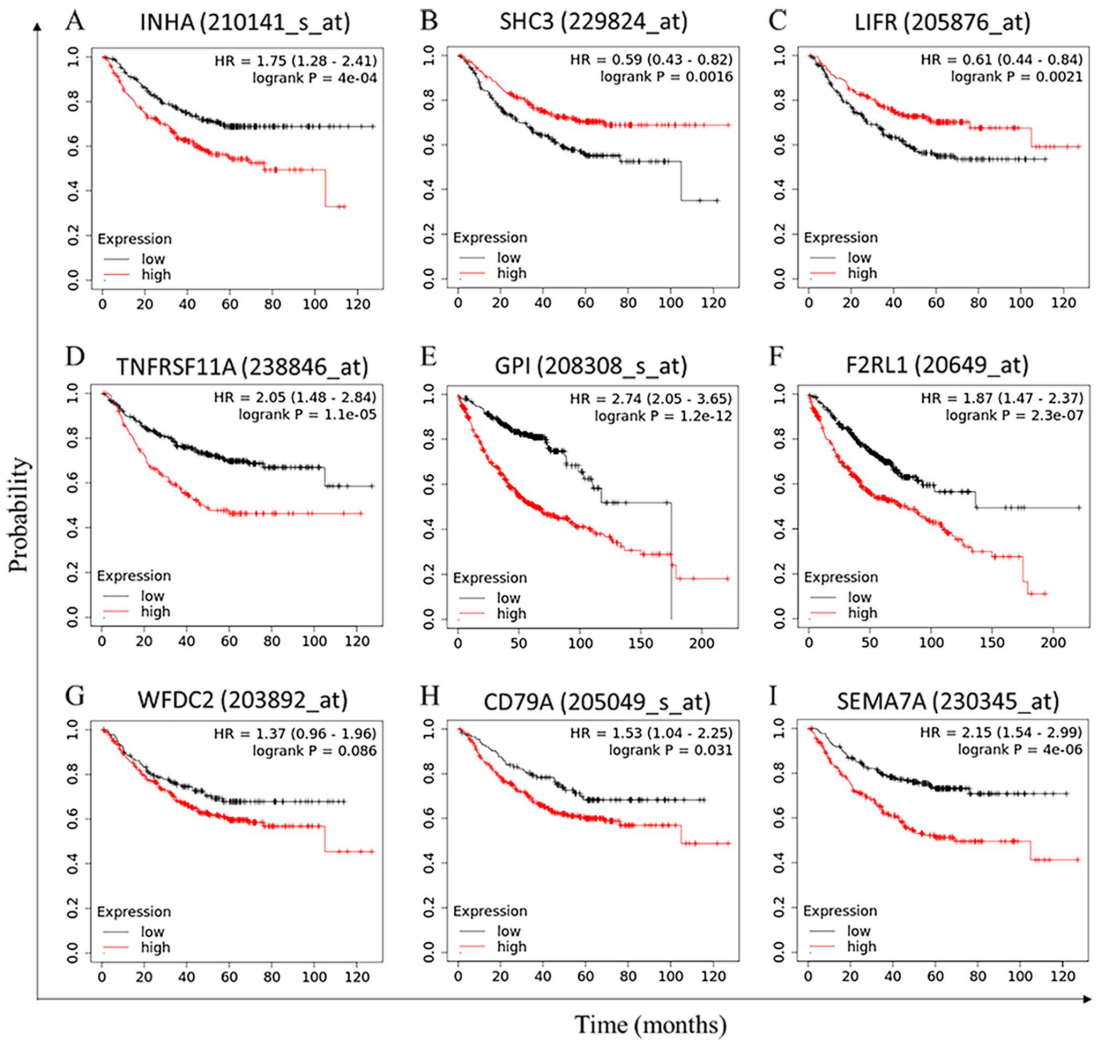

Figure S4. The prognostic value of nine signature genes for recurrence-free survival (RFS) was evaluated by Kaplan-Meier survival analysis. LUAD patients were subdivided into high/low gene expression groups according to the median expression level of each gene in LUAD tissues. RFS analysis of INHA (A), RFS analysis of SHC3 (B), RFS analysis of LIFR (C), RFS analysis of TNFRSF11A (D), RFS analysis of GPI (E), RFS analysis of F2RL1 (F), RFS analysis of WFDC2 (G), RFS analysis of CD79A (H) and RFS analysis of SEMA7A (I).

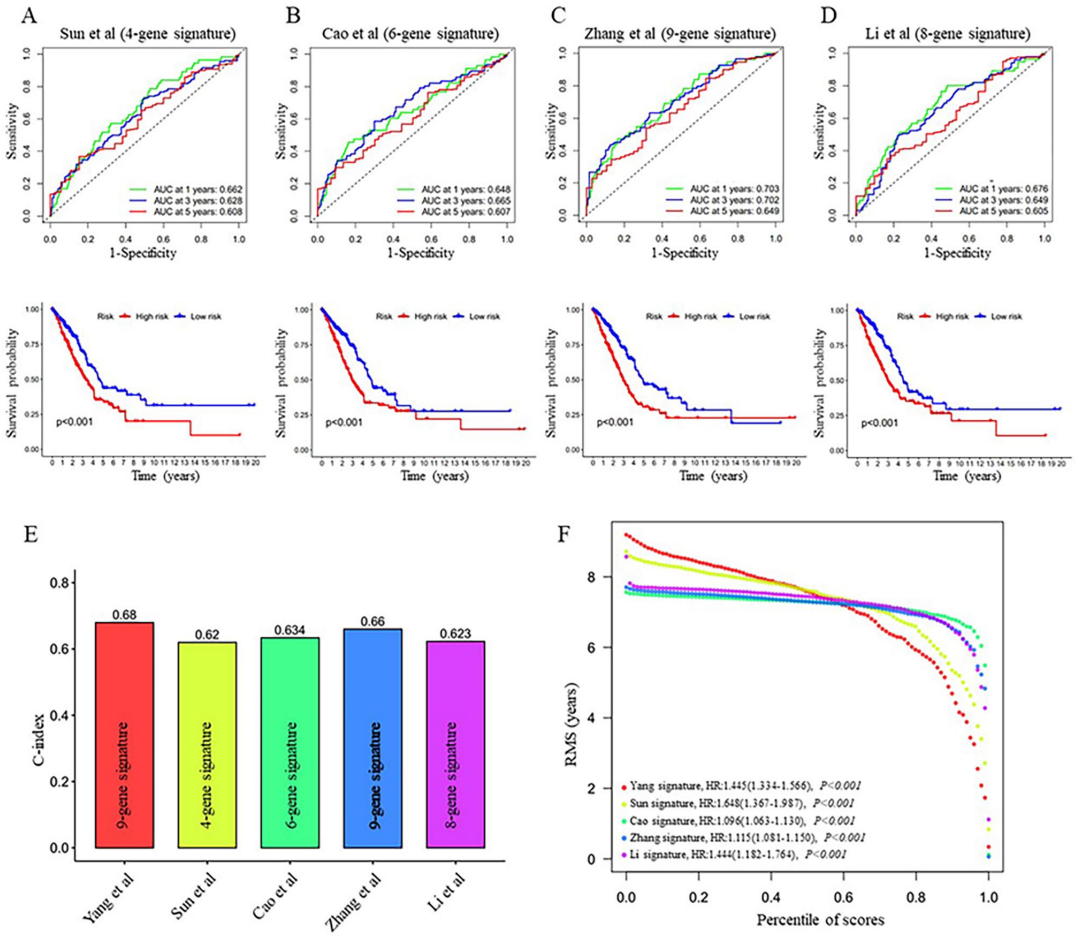

Figure S5. Comparison of the lrRIGs risk model with other reported risk models. (A-D) Time-dependent ROC and Kaplan-Meier curves analyses of four published gene signatures based on the TCGA_LUAD database. (E) Concordance index (C-index) of the five prognostic risk models, including our lrRIGs risk model (red histogram). (F) Restricted mean survival (RMS) time curves of all five risk models.

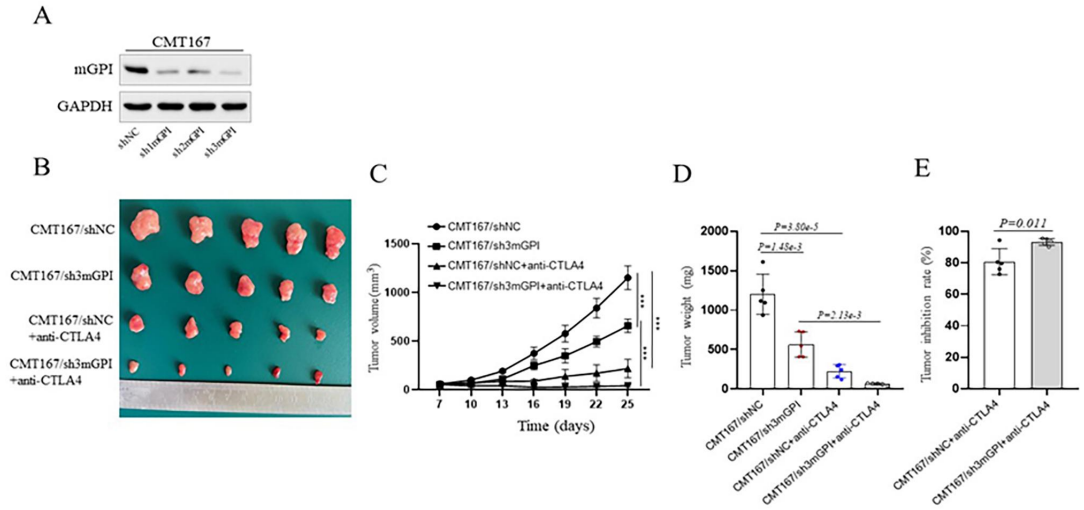

Figure S6. GPI knockdown improves anti-CTLA4 antibody therapy in the CMT167 model. (A) The Gpi1（mGPI）silencing efficiency of shRNA in CMT167 the cell line was examined by Western blotting. (B) CMT167/shNC or CMT167/sh3mGPI cells （2.5×105） were injected subcutaneously in the right flank of C57BL/6J mice (n=5/group). When tumors had reached a size of about 60 mm3, the mice were treated with anti-CTLA4 antibody (10mg/kg, every 3 days, i.v.) or PBS solution of the same volume. (C) The tumor volumes were measured at indicated time points. (D) The tumor weight of mice was measured. (E) The anti-tumor effects of anti-CTLA4 antibodies in the CMT167/shNC and CMT167/sh3mGPI groups were evaluated. Tumor volume = width2 × length × π/6; Tumor inhibition rate (%) = (1-tumor volume of treatment group/tumor volume of control group) × 100%. ***, P<0.001.

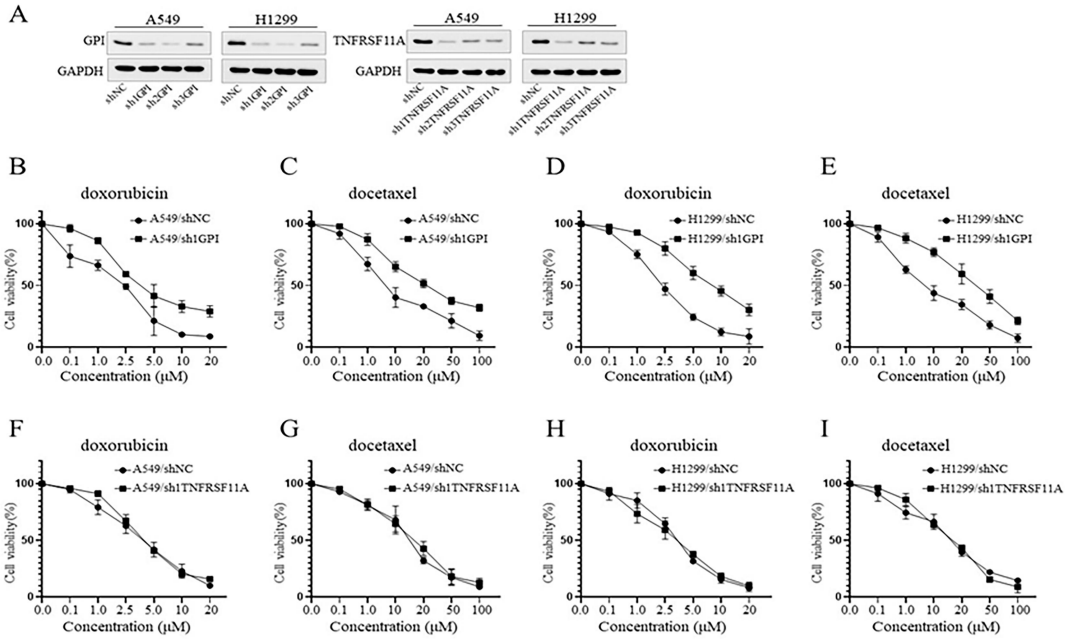

Figure S7. **Cytotoxicity of doxorubicin and docetaxel in control and GPI knockdown or TNFRSF11A knockdown cells.** The GPI and TNFRSF11A silencing efficiency of shRNA in A549 and H1299 cells were analyzed by Western blotting (A). A549 and H1299 cells were treated with indicated concentrations of doxorubicin (A, E, C, G) or docetaxel (B, D, F, H) for 24 hours. Cell viability was determined by the AlamarBlue assay (n=3). All measurements were conducted in triplicate and independently repeated three times.